

See discussions, stats, and author profiles for this publication at: <https://www.researchgate.net/publication/332792029>

# Properties and Limits of the Minimum-norm Differential Beamformers with Circular Microphone Arrays

Conference Paper · May 2019

DOI: 10.1109/ICASSP.2019.8683585

CITATIONS

0

READS

37

4 authors:



**Gongping Huang**

Technion - Israel Institute of Technology. הטכניון

24 PUBLICATIONS 94 CITATIONS

[SEE PROFILE](#)



**Xudong Zhao**

Northwestern Polytechnical University

1 PUBLICATION 0 CITATIONS

[SEE PROFILE](#)



**Jingdong Chen**

Institute of Electrical and Electronics Engineers

307 PUBLICATIONS 4,721 CITATIONS

[SEE PROFILE](#)



**Jacob Benesty**

Institut National de la Recherche Scientifique

613 PUBLICATIONS 12,800 CITATIONS

[SEE PROFILE](#)

Some of the authors of this publication are also working on these related projects:



Frequency-Invariant Beamforming [View project](#)



Array Processing--Kronecker Product Beamforming [View project](#)

# PROPERTIES AND LIMITS OF THE MINIMUM-NORM DIFFERENTIAL BEAMFORMERS WITH CIRCULAR MICROPHONE ARRAYS

Gongping Huang<sup>1</sup>, Xudong Zhao<sup>1</sup>, Jingdong Chen<sup>1</sup>, and Jacob Benesty<sup>2</sup>

<sup>1</sup>CIAIC  
Northwestern Polytechnical University  
Xi'an, Shaanxi 710072, China

<sup>2</sup>INRS-EMT, University of Quebec  
800 de la Gauchetiere Ouest, Suite 6900  
Montreal, QC H5A 1K6, Canada

## ABSTRACT

Small aperture circular microphone arrays (CMAs) have been widely used in many applications such as teleconferencing, smart-speakers, and robotics. A critical component of such arrays is the differential beamformer, which can achieve relatively high spatial gains with the same beampatterns at most frequencies. Among different differential beamforming approaches that were developed in the literature, the minimum-norm one has attracted much interest as it can deal better with sensors' self noise, sensor mismatch, and beamformer's irregularity at some frequencies due to the zeros of the Bessel functions. In our previous study, we have investigated the performance of the minimum-norm differential beamformer with uniform CMAs (UCMAs) in the 2-dimensional (2D) space where the sound sources and the sensors are assumed to be in the same plane. But in practice, this assumption is generally not true. So, in this paper, we investigate the properties and limitations of the minimum-norm differential beamformer in the 3-dimensional (3D) space. Through theoretical study as well as simulations, we show that the minimum-norm differential beamformer is effective in dealing with the problem of white noise amplification and irregularity of the beampatterns and the directivity factor (DF) if the steering angles are within or near the sensor plane, but it becomes less and less effective as the beamformer is steered away from this plane.

**Index Terms**— Microphone arrays, differential beamforming, uniform circular microphone arrays, frequency-invariant beampattern.

## 1. SIGNAL MODEL AND PROBLEM FORMULATION

Consider a uniform circular microphone array (UCMA) of radius  $r$ , which consists of  $M$  omnidirectional microphones. We assume that all the sensors are in a same plane. Without loss of generality, we assume that they are in the horizontal plane and the center of the UCMA coincides with the origin of the Cartesian coordinate system. The azimuth angles are measured anti-clockwise from the  $x$  axis and the first sensor (Sensor 1) of the array is placed on the  $x$  axis. The angular position of the  $m$ th array element is  $\psi_m = 2\pi(m-1)/M$ ,  $m = 1, 2, \dots, M$ . In a far-field and anechoic acoustic environment, the steering vector corresponding to a given steering angle  $\theta$  is [1,2]

$$\mathbf{d}(\omega, \theta) = [ e^{j\varpi \cos(\theta - \psi_1)} \quad \dots \quad e^{j\varpi \cos(\theta - \psi_M)} ]^T, \quad (1)$$

where the superscript  $T$  is the transpose operator,  $j$  is the imaginary unit with  $j^2 = -1$ ,  $\varpi = \omega r/c$ ,  $\omega = 2\pi f$  is the angular frequency,  $f > 0$  is the temporal frequency, and  $c = 340$  m/s is the speed of sound.

In linear beamforming, we apply a complex weight,  $H_m^*(\omega)$ , at the output of the  $m$ th microphone, where the superscript  $*$  is the complex conjugate, and then sum all the weighted outputs together

This work was supported in part by the National Natural Science Foundation of China (NSFC) under grant no. 61831019 and 61425005 and the NSFC and the Israel Science Foundation (ISF) joint research program under Grant No. 61761146001.

to form an estimate of the source signal. Stacking all these weights together, we get a vector of length  $M$ :

$$\mathbf{h}(\omega) = [ H_1(\omega) \quad H_2(\omega) \quad \dots \quad H_M(\omega) ]^T. \quad (2)$$

Now, the problem of beamforming is to find an optimal beamforming filter,  $\mathbf{h}(\omega)$ , by optimizing some cost function such as the DF or the mean-squared error (MSE) between the signal of interest and its estimate, so that the output of the beamformer is a good estimate of the desired signal. In this work, we adopt the approach in [3,4], where the optimal beamformer is derived by matching its beampattern to a specified target beampattern in the 2D space. The beampattern of  $\mathbf{h}(\omega)$ , which describes the sensitivity of the beamformer to a plane wave impinging on the array from the direction  $\theta$ , is written mathematically as [5–7]

$$\begin{aligned} \mathcal{B}[\mathbf{h}(\omega), \theta] &= \mathbf{h}^H(\omega) \mathbf{d}(\omega, \theta) \\ &= \sum_{m=1}^M H_m^*(\omega) e^{j\varpi \cos(\theta - \psi_m)}, \end{aligned} \quad (3)$$

where the superscript  $H$  is the conjugate-transpose operator.

Let us choose the frequency-invariant directivity pattern of an  $N$ th-order circular differential microphone array (CDMA) as the target beampattern. The beamforming problem is then transformed into one of finding the beamforming filter,  $\mathbf{h}(\omega)$ , so that  $\mathcal{B}[\mathbf{h}(\omega), \theta]$  is as close as possible to the directivity pattern of the given  $N$ th-order CDMA.

## 2. FREQUENCY-INVARIANT TARGET BEAMPATTERN

In this work, we choose the frequency-invariant directivity pattern of an  $N$ th-order CDMA as the target beampattern so that the resulting beamformer works as a differential beamformer. With its main beam pointing to the direction  $\theta_s$ , the  $N$ th-order frequency-invariant directivity pattern is given by [8]

$$\begin{aligned} \mathcal{B}(\mathbf{b}_{2N}, \theta - \theta_s) &= \sum_{n=-N}^N b_{2N,n} e^{j\varpi n(\theta - \theta_s)} \\ &= [\mathbf{\Upsilon}(\theta_s) \mathbf{b}_{2N}]^T \mathbf{p}_e(\theta) \\ &= \mathbf{c}_{2N}^T(\theta_s) \mathbf{p}_e(\theta) \\ &= \mathcal{B}[\mathbf{c}_{2N}(\theta_s), \theta], \end{aligned} \quad (4)$$

where  $b_{N,n}$ ,  $n = 0, \pm 1, \pm 2, \dots, \pm N$  are real coefficients and

$$\begin{aligned} \mathbf{b}_{2N} &= [ b_{2N,-N} \quad \dots \quad b_{2N,0} \quad \dots \quad b_{2N,N} ]^T, \\ \mathbf{\Upsilon}(\theta_s) &= \text{diag}(e^{jN\theta_s}, \dots, 1, \dots, e^{-jN\theta_s}), \\ \mathbf{p}_e(\theta) &= [ e^{-jN\theta} \quad \dots \quad 1 \quad \dots \quad e^{jN\theta} ]^T, \\ \mathbf{c}_{2N}(\theta_s) &= \mathbf{\Upsilon}(\theta_s) \mathbf{b}_{2N} \\ &= [ c_{2N,-N}(\theta_s) \quad \dots \quad c_{2N,0}(\theta_s) \quad \dots \quad c_{2N,N}(\theta_s) ]^T. \end{aligned}$$

The values of the  $b_{2N,n}$ 's in (4) determine the different directivity patterns of the  $N$ th-order CDMA, details of which can be found in [8]. In the direction of the main beam, i.e.,  $\theta = \theta_s$ , the directivity pattern should be equal to 1 so that the signal from this direction can pass through the beamformer undistorted, i.e.,

$$\mathcal{B}(\mathbf{b}_{2N}, 0) = \sum_{n=-N}^N b_{2N,n} = 1. \quad (5)$$

### 3. BEAMFORMING FILTER DESIGN VIA THE MINIMUM-NORM APPROACH

Following the method in [8], we attempt to find the beamforming filter,  $\mathbf{h}(\omega)$ , so that its beampattern,  $\mathcal{B}[\mathbf{h}(\omega), \theta]$ , is close to the target directivity pattern,  $\mathcal{B}(\mathbf{b}_{2N}, \theta - \theta_s)$ , i.e.,

$$\mathcal{B}[\mathbf{h}(\omega), \theta] = \mathcal{B}(\mathbf{b}_{2N}, \theta - \theta_s), \quad \forall \omega. \quad (6)$$

To solve the linear system in (6), we first apply the Jacobi-Anger expansion of order  $N$  to  $\mathcal{B}[\mathbf{h}(\omega), \theta]$  [8], [22], i.e.,

$$\begin{aligned} \mathcal{B}[\mathbf{h}(\omega), \theta] &= \sum_{m=1}^M H_m^*(\omega) e^{j\varpi \cos(\theta - \psi_m)} \\ &= \sum_{m=1}^M H_m^*(\omega) \sum_{n=-N}^N j^n J_n(\varpi) e^{jn(\theta - \psi_m)} \\ &= \sum_{n=-N}^N e^{jn\theta} \left[ \sum_{m=1}^M j^n J_n(\varpi) e^{-jn\psi_m} H_m^*(\omega) \right]. \end{aligned} \quad (7)$$

From (7) and (4), the relation between the designed beampattern and the target directivity pattern is found as

$$j^n J_n(\varpi) \sum_{m=1}^M e^{-jn\psi_m} H_m^*(\omega) = c_{2N,n}(\theta_s). \quad (8)$$

Then, it follows that

$$\Psi \mathbf{h}(\omega) = \mathbf{J}^*(\varpi) \mathbf{c}_{2N}^*(\theta_s), \quad (9)$$

where

$$\Psi = \begin{bmatrix} \psi_{-N}^H \\ \vdots \\ \psi_0^H \\ \vdots \\ \psi_N^H \end{bmatrix} \quad (10)$$

is a  $(2N+1) \times M$  matrix, with

$$\psi_n = [e^{-jn\psi_1} \quad e^{-jn\psi_2} \quad \dots \quad e^{-jn\psi_M}]^T, \quad (11)$$

$n = 0, \pm 1, \pm 2, \dots, \pm N$ , and

$$\mathbf{J}(\varpi) = \text{diag} \left[ \frac{j^N}{J_{-N}(\varpi)}, \dots, \frac{1}{J_0(\varpi)}, \dots, \frac{j^{-N}}{J_N(\varpi)} \right] \quad (12)$$

is a  $(2N+1) \times (2N+1)$  diagonal matrix. Generally, to design an  $N$ th-order CDMA, at least  $2N+1$  microphones are needed. If  $2N+1$  microphones are used, it is not difficult to check that  $\Psi \Psi^H = M \mathbf{I}_M$ , so  $\Psi^{-1} = \Psi^H/M$ . Then, the solution of (9) is

$$\begin{aligned} \mathbf{h}_D(\omega) &= \Psi^{-1} \mathbf{J}^*(\varpi) \mathbf{c}_{2N}^*(\theta_s) \\ &= \frac{1}{M} \Psi^H \mathbf{J}^*(\varpi) \Upsilon^*(\theta_s) \mathbf{b}_{2N}, \end{aligned} \quad (13)$$

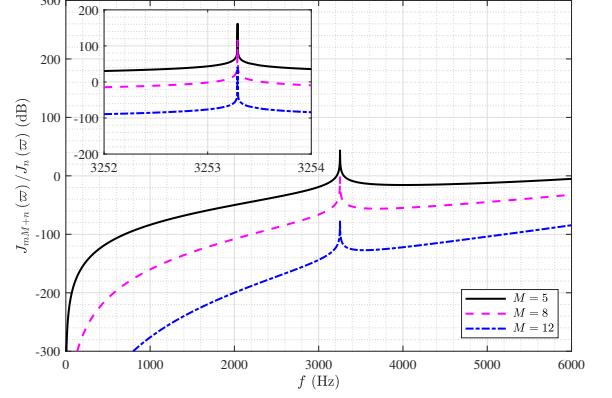


**Fig. 1.**  $J_{mM+n}(\varpi)/J_n(\varpi)$  as a function of the frequency,  $f$ , for different numbers of microphones. Conditions:  $r = 4.0$  cm,  $m = 1$ , and  $n = 0$ .

where the subscript  $D$  stands for the direct inverse. But this solution is in general sensitive to the sensors' self noise and mismatch among sensors. To improve the robustness, we typically increase the number of microphones, i.e.,  $M > 2N+1$ . In this case, we obtain the minimum-norm solution of (9) [8], i.e.,

$$\begin{aligned} \mathbf{h}_{MN}(\omega) &= \Psi^H (\Psi \Psi^H)^{-1} \mathbf{J}^*(\varpi) \mathbf{c}_{2N}^*(\theta_s) \\ &= \frac{1}{M} \Psi^H \mathbf{J}^*(\varpi) \Upsilon^*(\theta_s) \mathbf{b}_{2N}. \end{aligned} \quad (14)$$

### 4. PERFORMANCE STUDY AND ANALYSIS

The minimum-norm beamformer developed in Section 3, which was originally derived in [8] is based on a 2D space where the sound sources and sensors are assumed to be in a same plane. It was shown in [8] that the robustness of this beamformer with respect to sensors' self noise increases with the number of microphones. In other words, the more the microphones, the higher is the white noise gain. However, in practice, the sensors and the sound sources are generally not in the same plane. It is therefore important to analyze the performance of this beamformer in the 3D space. For this purpose, let us first extend the 2D beampattern to the 3D space by including the elevation angle, i.e.,

$$\mathcal{B}[\mathbf{h}_{MN}(\omega), \phi, \theta] = \sum_{m=1}^M H_m^*(\omega) e^{j\varpi \sin \phi \cos(\theta - \psi_m)}, \quad (15)$$

where  $\phi$  is the elevation angle. Clearly, (15) degenerates to (3) if  $\phi = \pi/2$ . Now, substituting (14) into (15), we get

$$\begin{aligned} \mathcal{B}[\mathbf{h}_{MN}(\omega), \phi, \theta] &= \sum_{m=1}^M H_m^*(\omega) \sum_{l=-\infty}^{\infty} e^{jl\theta} j^l J_l(\varpi \sin \phi) e^{jl(\theta - \psi_m)} \\ &= \sum_{l=-\infty}^{\infty} e^{jl\theta} j^l J_l(\varpi \sin \phi) \psi_l^T \mathbf{h}_{MN}^*(\omega) \\ &= \frac{1}{M} \sum_{l=-\infty}^{\infty} e^{jl\theta} j^l J_l(\varpi \sin \phi) \psi_l^T \Psi^T \mathbf{J}(\varpi) \mathbf{c}_{2N}(\theta_s). \end{aligned} \quad (16)$$

Using the fact that  $\psi_l^T \Psi^T = \mathbf{0}$  for  $l \neq mM + n$  with  $m \geq 0$  and  $n = 0, \pm 1, \pm 2, \dots, \pm N$ , we have

$$\begin{aligned} \mathcal{B}[\mathbf{h}_{MN}(\omega), \phi, \theta] &= \sum_{m=0}^{\infty} j^{mM} e^{jmM\theta} \sum_{n=-N}^N \frac{J_{mM+n}(\varpi \sin \phi)}{J_n(\varpi)} e^{jm\theta} c_{2N,n}(\theta_s) \\ &= \sum_{n=-N}^N e^{jm\theta} c_{2N,n}(\theta_s) \frac{J_n(\varpi \sin \phi)}{J_n(\varpi)} + \sum_{m=1}^{\infty} j^{mM} e^{jmM\theta} \\ &\quad \times \sum_{n=-N}^N \frac{J_{mM+n}(\varpi \sin \phi)}{J_n(\varpi)} e^{jm\theta} c_{2N,n}(\theta_s). \end{aligned} \quad (17)$$

Now, we consider the following two cases.

- $\phi = \pi/2$ . This case corresponds to the horizontal plane. In this scenario, the first part of the right-hand side of (17) is equal to the target directivity pattern  $\mathcal{B}[c_{2N}(\theta_s), \theta]$ , and the second part can be viewed as an approximation error between the obtained beampattern and the target directivity pattern. So, we have

$$\begin{aligned} \epsilon_{\mathcal{B}[\mathbf{h}_{MN}(\omega), \theta]} &= \mathcal{B}[\mathbf{h}_{MN}(\omega), \theta] - \mathcal{B}[c_{2N}(\theta_s), \theta] \\ &= \sum_{n=-N}^N \frac{c_{2N,n}(\theta_s)}{j^n} \sum_{m=1}^{\infty} e^{j(mM+n)(\theta+\frac{\pi}{2})} \frac{J_{mM+n}(\varpi)}{J_n(\varpi)}. \end{aligned} \quad (18)$$

As seen, the value of the approximation error is mainly influenced by the term  $J_{mM+n}(\varpi)/J_n(\varpi)$ . Generally, the value of  $J_{mM+n}(\varpi)/J_n(\varpi)$  depends on the frequency  $\varpi$ , the number of microphones  $M$ , and the order  $n$ . Figure 1 plots an example of  $J_{mM+n}(\varpi)/J_n(\varpi)$  as a function of the frequency with  $m = 1$ ,  $n = 0$ ,  $r = 4.0$  cm, and  $M \in \{5, 8, 12\}$ . As seen, the value of  $J_{mM+n}(\varpi)/J_n(\varpi)$  decreases significantly as the value of  $M$  increases. Therefore, the approximation error is greatly reduced by increasing the number of microphones. In other words, the robustness of the minimum-norm beamformer can be greatly improved by increasing the number of sensors. We notice that there is a narrow peak with each curve in Fig. 1. The peak in the three curves happens at the frequency where  $J_n(\varpi)$  is close to 0. From the zoomed plot of the portion near the peak, one can see that the value of the peak is very large regardless of the number of sensors. To avoid this large error, we have to adjust the aperture of the array besides the number of sensors.

- $\phi \neq \pi/2$ . In this case, the distortion consists of two parts: the approximation error (same as before), and the projection error coming from the term  $J_n(\varpi \sin \phi)/J_n(\varpi)$ . Similarly, the approximation error decreases significantly as the value of  $M$  increases. So, as long as we use sufficient number of microphone sensors, the approximation error can be ignored. However, the term  $J_n(\varpi \sin \phi)/J_n(\varpi)$  is a function of  $\varpi$  and  $\phi$ , but it does not depend on  $M$ . As a result, increasing the number of microphones, i.e., increasing the value of  $M$ , would have no effect on this error. This indicates that the minimum-norm method becomes less effective in dealing with the robustness problem as the steering angle moves away from the sensors' plane.

## 5. SIMULATIONS

In this section, we continue to study and analyze the performance of the minimum-norm beamformer through simulations. The performance is evaluated using the three widely used metrics, i.e., beampattern, directivity factor (DF), and white noise gain (WNG) [6]. The microphone array used is a UCMA with a radius of  $r$  and  $M$  microphones. In all simulations, the target directivity pattern is set to the

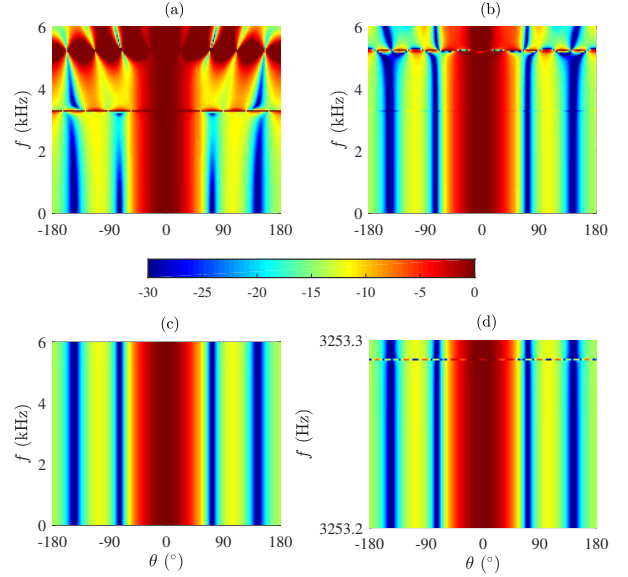


**Fig. 2.** Beampatterns of the minimum-norm beamformer with UCMA: (a)  $M = 5$ , (b)  $M = 8$ , (c)  $M = 12$ , and (d) zoomed plot of the beampatterns of  $M = 12$ . Conditions:  $r = 4.0$  cm

second-order hypercardioid with its main beam pointing to  $0^\circ$  [6], i.e.,  $\theta_s = 0^\circ$ . The coefficients  $\mathbf{b}_{2N}$  of this beamformer are given by [8]

$$\mathbf{b}_{2N} = [0.2 \ 0.2 \ 0.2 \ 0.2 \ 0.2]^T. \quad (19)$$

Conventionally, the DF is defined as the ratio between the magnitude squared beampattern in the look direction and the averaged magnitude squared beampattern over the entire space [6, 20]. To better visualize the performance in different planes that are parallel to the sensors' plane, we define here the 2D DF, which is a function of the elevation angle  $\phi$  [10]:

$$\mathcal{D}[\mathbf{h}_{MN}(\omega), \phi] = \frac{2\pi |\mathcal{B}[\mathbf{h}_{MN}(\omega), \phi, \theta_s]|^2}{\int_0^{2\pi} |\mathcal{B}[\mathbf{h}_{MN}(\omega), \phi, \theta]|^2 d\theta} \quad (20)$$

The WNG quantifies the sensitivity of a beamformer to some of the array's imperfections such as sensors' self noise and mismatch among sensors. According to [10, 23], the WNG is written as

$$\mathcal{W}[\mathbf{h}_{MN}(\omega)] = \frac{|\mathbf{h}_{MN}^H(\omega) \mathbf{d}(\omega, \theta_s)|^2}{\mathbf{h}_{MN}^H(\omega) \mathbf{h}_{MN}(\omega)}. \quad (21)$$

Figure 2 plots the beampatterns of the minimum-norm beamformer in the sensor plane (i.e.,  $\phi = \pi/2$ ) with  $r = 4.0$  cm, for  $M \in \{5, 8, 12\}$ . As seen, the beampattern is considerably distorted at high frequencies due to the so-called null problem (see [8]) with  $M = 5$ ; but the distortion becomes less and less serious as the number of sensors increases. With  $M = 12$ , it is seen from Fig. 2 (c) that the beampatterns of the minimum-norm beamformer is almost frequency invariant in the studied frequency range, which demonstrates the property of the minimum-norm approach, i.e., it can take advantage of the redundancy among the additional microphones to improve the robustness of the beamformer. However, as discussed previously, the null problem may still exist, as shown in the zoomed plot of a portion of Fig. 2(c) in Fig. 2 (d). In other words, as the number of microphones increases, the deep null problem may still exist, but it only happens in a narrow frequency range, which is negligible in practice as the frequency resolution is limited in algorithm implementation. This corroborates the result in Fig. 1, where we have shown that the deep nulls may always exist; but they can be avoided with limited frequency resolution in practical implementation.

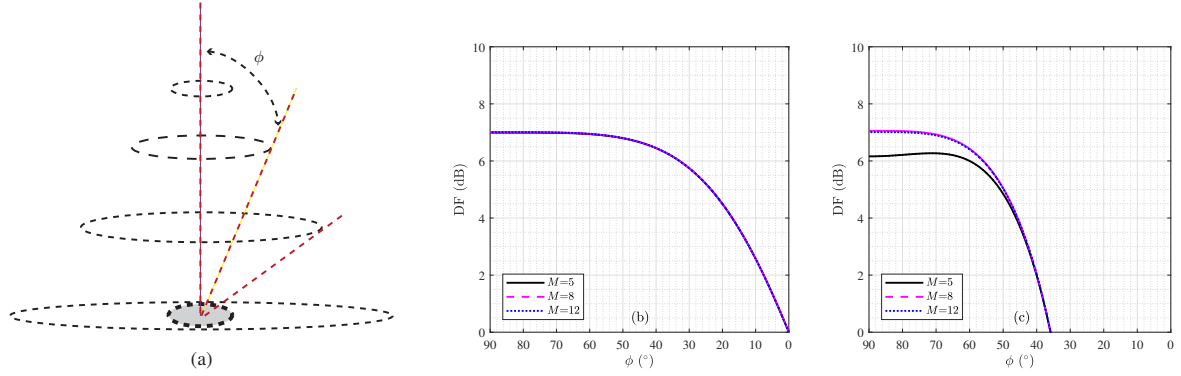


**Fig. 3.** DF of the minimum-norm beamformer with UCMA as a function of  $\phi$  for different numbers of microphones: (a) illustration of different parallel planes, (b) DF at  $f = 1$  kHz, and (c) DF at  $f = 4$  kHz. Conditions:  $r = 4.0$  cm.

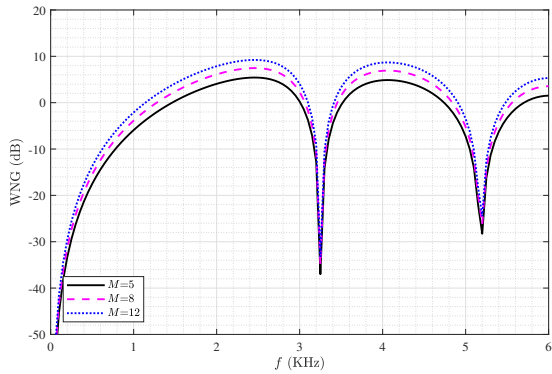


**Fig. 4.** WNG of the minimum-norm beamformer with UCMA as a function of the frequency,  $f$ , for different numbers of microphones. Conditions:  $r = 4.0$  cm.

To illustrate the beamforming performance on different planes, Fig. 3 plots the DF of the minimum-norm beamformer as a function of the elevation angle,  $\phi$ , with  $r = 4.0$  cm and  $M \in \{5, 8, 12\}$ . For each elevation angle,  $\phi$ , we compute the corresponding beampattern and the DF is subsequently computed according to (20). It is seen that the DF decreases as the value of  $\phi$  decreases from  $90^\circ$  to  $0^\circ$ .

Figure 4 plots the WNG of the minimum-norm beamformer as a function of the frequency with  $M \in \{5, 8, 12\}$ . It is clearly seen that the WNG suffers from significant deep nulls at some frequencies. With the minimum-norm method, increasing the number of microphones can improve the WNG at most frequencies; but the problem of nulls still exists. This indicates that while it can help improve the WNG, the minimum-norm approach cannot eliminate the null problem of WNG. As a matter of fact, with the beamforming filter in (13), it is not difficult to verify that

$$\mathcal{W}[\mathbf{h}_{\text{MN}}(\omega)] = \frac{M |\mathbf{h}_{\text{MN}}^H(\omega) \mathbf{d}(\omega, \theta_s)|^2}{\sum_{n=-N}^N \frac{b_{2N,n}^2}{J_n^2(\varpi)}}. \quad (22)$$

As seen, the zeros of the Bessel function in the denominator does not depend on  $M$ . As a result, increasing the value of  $M$  does not affect the nulls of WNG. But for a fixed value of the order  $N$ , one can improve the WNG by increasing the value of  $M$ , i.e., the number of sensors, for frequencies where the denominator of (22) is not close to zero.

## 6. CONCLUSIONS

The minimum-norm beamformer with CMAs has attracted much interest as its robustness with respect to sensors' self noise, mismatch

among sensors, etc, improves as the number of sensors increases. Previous analysis on the performance of the minimum-norm beamformer was focused on the 2D space with the assumption that the sound sources and the sensors are in the same plane. In this paper, we studied the performance of the minimum-norm beamformer in a more general 3D space. By analyzing the error between the beampattern of the minimum-norm beamformer and the target beampattern, we showed that the minimum-norm differential beamformer is effective in dealing with the problem of white noise amplification and irregularity of the beampatterns and the DF if the steering angle is within or near the sensor plane, but the improvement becomes less and less significant as the beamformer is steered away from the sensor plane. Simulations were performed and the results verified the theoretical analysis.

## 7. RELATION TO PRIOR WORK

Beamforming is widely used in microphone array systems to recover a sound signal of interest from its noisy observations. Many beamforming algorithms have been proposed in the literature [5, 9–19]. Among those, differential beamformers are very attractive in applications using small-aperture arrays as they can achieve relatively high directional gains with consistent beampatterns across a wide range of frequencies [6, 20]. To achieve full steering flexibility, circular microphone arrays (CMAs) are often used [7, 8, 21]. However, differential beamforming with CMAs often suffers from white noise amplification at low frequencies and deep nulls in both WNG and DF at some frequencies where the values of the Bessel functions approach to zero [3, 4]. One way to deal with this null problem is by using concentric CMAs (CCMAs) with more than one ring [3, 4], but this would require more microphone sensors and large array aperture, which may not be feasible in applications where cost and size are restricted. Another way is by increasing the number of microphones while fixing the order of differential beamformer and the aperture of the array (in this case, the DF is unchanged). In our previous work, we have investigated the performance and properties of this method [7, 8] in the 2D space where the sound sources and the sensors are assumed to be in the same plane (e.g., the horizontal plane). However, in many really applications such as smart speakers and teleconferencing systems, sound sources (either desired, interference, or noise) and sensors are often not in the same plane. Therefore, it is important to examine the performance behavior of the minimum-norm beamformer in a general 3D space. By analyzing the error between the designed beampattern and the target one in the 3D space, we show that the minimum-norm differential beamformer is effective in dealing with the problem of white noise amplification and irregularity of the beampatterns and the DF if the steering angle is within or near the sensor plane, but it becomes less and less effective as the beamformer is steered away from the sensor plane.

## 8. REFERENCES

- [1] R. A. Monzingo and T. W. Miller, *Introduction to Adaptive Arrays*. SciTech Publishing, Inc, Raleigh, NC, 2004.
- [2] H. L. Van Trees, *Detection, Estimation, and Modulation Theory, Optimum Array Processing*. John Wiley & Sons, 2004.
- [3] G. Huang, J. Chen, and J. Benesty, "On the design of differential beamformers with arbitrary planar microphone array," *J. Acoust. Soc. Am.*, vol. 144, no. 1, pp. 3024–3035, 2018.
- [4] G. Huang, J. Chen, and J. Benesty, "Insights into frequency-invariant beamforming with concentric circular microphone arrays," *IEEE/ACM Trans. Audio, Speech, Lang. Process.*, vol. 26, no. 12, pp. 2305–2318, 2018.
- [5] J. Benesty, J. Chen, and Y. Huang, *Microphone Array Signal Processing*. Berlin, Germany: Springer-Verlag, 2008.
- [6] J. Benesty and J. Chen, *Study and Design of Differential Microphone Arrays*. Berlin, Germany: Springer-Verlag, 2012.
- [7] J. Benesty, J. Chen, and I. Cohen, *Design of Circular Differential Microphone Arrays*. Berlin, Germany: Springer-Verlag, 2015.
- [8] G. Huang, J. Benesty, and J. Chen, "On the design of frequency-invariant beampatterns with uniform circular microphone arrays," *IEEE/ACM Trans. Audio, Speech, Lang. Process.*, vol. 25, no. 5, pp. 1140–1153, 2017.
- [9] G. W. Elko and J. Meyer, "Microphone arrays," in *Springer Handbook of Speech Processing* (J. Benesty, M. M. Sondhi, and Y. Huang, eds.), ch. 48, pp. 1021–1041, Berlin, Germany: Springer-Verlag, 2008.
- [10] G. W. Elko, "Superdirectional microphone arrays," in *Acoustic Signal Processing for Telecommunication*, pp. 181–237, Springer, 2000.
- [11] B. Rafaely, *Fundamentals of Spherical Array Processing*. Berlin, Germany: Springer-Verlag, 2015.
- [12] S. Markovich-Golan, S. Gannot, and W. Kellermann, "Combined LCMV-tricon beamforming for separating multiple speech sources in noisy and reverberant environments," *IEEE/ACM Trans. Audio, Speech, Lang. Process.*, vol. 25, pp. 320–332, 2016.
- [13] T. D. Abhayapala and A. Gupta, "Higher order differential-integral microphone arrays," *J. Acoust. Soc. Am.*, vol. 136, pp. 227–233, May 2010.
- [14] E. Tiana-Roig, F. Jacobsen, and E. F. Grande, "Beamforming with a circular microphone array for localization of environmental noise sources," *J. Acoust. Soc. Am.*, vol. 128, no. 6, pp. 3535–3542, 2010.
- [15] S. Yan, Y. Ma, and C. Hou, "Optimal array pattern synthesis for broadband arrays," *J. Acoust. Soc. Am.*, vol. 122, no. 5, pp. 2686–2696, 2007.
- [16] D. Marquardt, E. Hadad, S. Gannot, and S. Doclo, "Theoretical analysis of linearly constrained multi-channel wiener filtering algorithms for combined noise reduction and binaural cue preservation in binaural hearing aids," *IEEE/ACM Trans. Audio, Speech, Lang. Process.*, vol. 23, no. 12, pp. 2384–2397, 2015.
- [17] G. Huang, J. Chen, and J. Benesty, "A flexible high directivity beamformer with spherical microphone arrays," *J. Acoust. Soc. Am.*, vol. 143, no. 5, pp. 3024–3035, 2018.
- [18] G. Huang, J. Benesty, and J. Chen, "Superdirective beamforming based on the Krylov matrix," *IEEE/ACM Trans. Audio, Speech, Lang. Process.*, vol. 24, pp. 2531–2543, 2016.
- [19] E. Messner, H. Pessentheiner, J. A. Morales-Cordovilla, and M. Hagmüller, "Adaptive differential microphone arrays used as a front-end for an automatic speech recognition system," in *Proc. IEEE ICASSP*, pp. 2689–2693, IEEE, 2015.
- [20] G. W. Elko, "Differential microphone arrays," in *Audio Signal Processing for Next-Generation Multimedia Communication Systems*, pp. 11–65, Springer, 2004.
- [21] G. Huang, J. Benesty, and J. Chen, "Design of robust concentric circular differential microphone arrays," *J. Acoust. Soc. Am.*, vol. 141, no. 5, pp. 3236–3249, 2017.
- [22] M. Abramowitz and I. A. Stegun, *Handbook of Mathematical Functions: with Formulas, Graphs, and Mathematical Tables*, vol. 55. Dover Publications, New York, NY, 1965.
- [23] M. Brandstein and D. Ward, *Microphone Arrays: Signal Processing Techniques and Applications*. Springer, 2001.